Geophysical Research Letters

RESEARCH LETTER
10.1029/2019GL082787

# A Multivariate AMV Index and Associated Discrepancies Between Observed and CMIP5 Externally Forced AMV

Xiaoqin Yan[1], Rong Zhang[2], and Thomas R. Knutson[2]

[1]The Program in Atmospheric and Oceanic Sciences, Princeton University, Princeton, NJ, USA, [2]NOAA/GFDL, Princeton, NJ, USA

**Key Points:**
- Observed AMV exhibits strong coherent variability that is unique to the Atlantic after removal of the signal regressed on global mean SST
- The CMIP5 multimodel mean forced AMV, after removal of the signal regressed on global mean SST, shows little resemblance to observed AMV
- Our study, which includes a novel multivariate AMV analysis, suggests that the observed AMV is not dominated by external forcing

**Supporting Information:**
- Supporting Information S1

**Correspondence to:**
X. Yan and R. Zhang,
xiaoqiny@princeton.edu;
rong.zhang@noaa.gov

**Citation:**
Yan, X., Zhang, R., & Knutson, T. R. (2019). A multivariate AMV index and associated discrepancies between observed and CMIP5 externally forced AMV. *Geophysical Research Letters*, *46*, 4421–4431. https://doi.org/10.1029/2019GL082787

Received 11 MAR 2019
Accepted 3 APR 2019
Accepted article online 5 APR 2019
Published online 23 APR 2019



**Abstract** Atlantic Multidecadal Variability (AMV) is a multivariate phenomenon. Here for the first time we obtain a multivariate AMV index and associated patterns using Multivariate Empirical Orthogonal Function (MEOF) analysis to explore the multivariate nature of AMV. Coherent multidecadal variability that is unique to the Atlantic is found in the observed MEOF-extracted AMV, various AMV-related indices, and an Atlantic Meridional Overturning Circulation fingerprint. When the signal associated with global mean sea surface temperature is removed from both observations and Coupled Model Intercomparison Project Phase 5 (CMIP5) simulations, the residual CMIP5 forced basin-wide sea surface temperature-based AMV index disagrees strongly with the observed residual. Only the observed residual basin-wide sea surface temperature-based AMV index retains a strong AMV signal. The MEOF approach still extracts a residual CMIP5 forced AMV signal that is unique to the Atlantic, although very different from observations. Our findings suggest that the observed AMV is not dominated by external forcing.

**Plain Language Summary** Observed Atlantic Multidecadal Variability is a multivariate phenomenon and has various important climate impacts at global and regional scales. Understanding the underlying physical mechanism is crucial for successful future prediction of Atlantic Multidecadal Variability and associated climate impacts. From a multivariate perspective, this study shows that the simulated externally forced Atlantic Multidecadal Variability in coupled climate model simulations disagrees strongly with that observed. The results suggest that the observed Atlantic Multidecadal Variability, after removal of the signal associated with global mean sea surface temperature, is not dominated by external forcing. This observed variability is unique to the Atlantic and is linked to multidecadal variations of the Atlantic Meridional Overturning Circulation.

## 1. Introduction

The leading mechanism of the observed Atlantic multidecadal variability (AMV) is often thought to be linked to the low-frequency variability of the Atlantic Meridional Overturning Circulation (AMOC; e.g., Ba et al., 2013, 2014; Delworth & Mann, 2000; Delworth et al., 2017; Drews & Greatbatch, 2016, 2017; Kim, Yeager, Chang, et al., 2018; Kim, Yeager, & Danabasoglu, 2018; Knight et al., 2005; Kushnir, 1994; Latif et al., 2006; McCarthy et al., 2015; Park et al., 2016; Yan et al., 2017, 2018; Zhang, 2017; Zhang et al., 2013, 2016). However, some recent studies suggest that AMV is mainly a direct response of the North Atlantic sea surface temperature (SST) to changes in external radiative forcings (e.g., Bellomo et al., 2018; Bellucci et al., 2017; Booth et al., 2012; Murphy et al., 2017). The conclusion of these recent studies is often based on the resemblance of the traditional basin-wide SST-based AMV index (i.e., the linearly detrended low-pass filtered SST anomalies averaged over the North Atlantic; Enfield et al., 2001) between the observation and the externally forced response in some historical climate simulations.

The linear detrending used in these studies does not cleanly separate AMV from the global scale signal, and it is important to remove the signal associated with global mean SST to obtain AMV (e.g., Frajka-Williams et al., 2017; Frankignoul et al., 2017; Sutton et al., 2018; Trenberth & Shea, 2006). As shown in R. Zhang et al. (2013), the simulated externally forced multidecadal SST signal in Booth et al. (2012) is not unique to the Atlantic, but also appears in many other ocean basins and represents a global scale response to external forcings. Additionally, the observed AMV is associated with coherent multidecadal variations in the subpolar North Atlantic (SPNA) SST, sea surface salinity (SSS), and upper ocean heat/salt content (UOHC/UOSC; e.g., Chen & Tung, 2014, 2018; Friedman et al., 2017; Kavvada et al., 2013; Robson et al., 2012, 2016; Wang et al., 2010; Yan et al., 2018; Yeager & Danabasoglu, 2014; Zhang, 2007, 2017; Zhang et al.,

2013). The externally forced response of the historical climate simulations does not capture well the observed multidecadal SSS variations in the SPNA that are coherent with the observed AMV (Bellucci et al., 2017; Zhang et al., 2013).

The observed AMV is a multivariate phenomenon that should be treated as a multivariate system. The Multivariate Empirical Orthogonal Function (MEOF) analysis has been used in studies of multivariate systems (e.g., Fukumori & Wunsch, 1991; Kutzbach, 1967; Sparnocchia et al., 2003; Wolter & Timlin, 1998, 2011) and applied to obtain a Multivariate El Niño/Southern Oscillation Index (MEI) to provide a more complete description of El Niño/Southern Oscillation (e.g., Wolter & Timlin, 1998, 2011). Here we apply MEOF analysis to obtain a Multivariate AMV Index (MAI), which is defined as the normalized leading principal component of the combined annual mean detrended anomalies of four AMV-related variables (SST, SSS, UOHC, and UOSC) over the North Atlantic to reflect the multivariate nature of AMV. Because the high coherences among the above four AMV-related variables only occur at low frequency and not at high frequency (Zhang, 2017), the MEOF approach has the advantage of extracting AMV without low-pass filtering.

The purpose of this study is to explore whether a comparison of the Coupled Model Intercomparison Project Phase 5 (CMIP5) multimodel mean (MMM) external forcing response with observations supports the hypothesis that the observed AMV is essentially externally forced. The comparison includes MAI and associated spatial patterns, multiple AMV-related indices, and multidecadal AMOC variability. Both linear detrending and nonlinear detrending (i.e., a residual signal is obtained by removing the component regressed on global mean SST anomalies from each variable) are applied. Removal of the component associated with global mean SST is not aimed at removing the externally forced signal as was the focus of several recent studies (e.g., Frankcombe et al., 2015; Kajtar et al., 2019). For example, the component regressed on global mean SST could have internal variability as well as externally forced contributions. Further, the remaining AMV after such removal could still retain an externally forced local component. Our results demonstrate that linear detrending is misleading and should be avoided in obtaining AMV from CMIP5 forced simulations and that the resemblance between linearly detrended observed and CMIP5 forced basin-wide SST-based AMV indices is an artifact of linear detrending. When the signal associated with global mean SST is removed to obtain the AMV, such resemblance disappears.

## 2. Data and Methods

Here the observed annual mean SSS and 0–700 m UOHC/UOSC are derived from the objectively analyzed temperature and salinity Ishii data set (Ishii et al., 2006) covering the period 1945–2012, and the observed annual mean SST for the same period is from the Hadley Centre sea ice and SST data set (Rayner et al., 2003). We compare observations with the externally forced response in CMIP5 simulations (see supporting information Table S1 for model information) over the same period, which is derived from their All-Forcing historical simulations (up to 2005) and extended through 2012 using the corresponding Representative Concentration Pathway 4.5 emission scenario simulations. The MMM represents the average CMIP5 forced response to changes in external forcings.

For the MEOF analysis, we normalize each variable with a constant (e.g., the square root of its total variance) to have equal unit total variance for each variable before computing the MEOF, similar to the approach used in Wolter and Timlin (2011). The constant is then multiplied back to the spatial pattern of each variable after computing the MEOF. The observed and CMIP5 MMM variables (i.e., SST, SSS, UOHC, and UOSC) are detrended before the MEOF analysis and no low-pass filtering are applied.

For comparison, we calculated multiple AMV-related indices for both observations and the CMIP5 MMM, that is, the 10-year low-pass filtered SST/SSS/UOHC/UOSC averaged over the SPNA (50–65°N, 60°W–0°) and the 10-year low-pass filtered SST averaged over the North Atlantic (0–65°N, 80°W–0°) (basin-wide SST-based AMV index). Due to the limitation of direct AMOC observations before 2004 (Smeed et al., 2014, 2018), we derived an extratropical AMOC fingerprint, a previously identified proxy for AMOC anomalies, to compare its relationship with the MAI. Here the AMOC fingerprint is defined as the leading mode of detrended annual mean 0–700 m UOHC in the extratropical North Atlantic (20–65°N, 80°W–0°E; Joyce & Zhang, 2010; Yan et al., 2017, 2018; Zhang, 2008, 2017; Zhang & Zhang, 2015). The CMIP5 externally forced AMOC Index, that is, the maximum Atlantic meridional overturning streamfunction at 26°N, is also

calculated from the MMM. The statistical significance for each correlation between a pair of time series is tested by a Monte Carlo simulation using a random phase resampling (Ebisuzaki, 1997).

## 3. MAI and Associated Spatial Patterns Under Linear Detrending

With linear detrending, the observed MAI is associated with a cooling/freshening in the SPNA during its negative phase from 1970s to 1990s and vice versa during its positive phases before and afterward (Figures 1a–1e). The observed SST anomalies associated with MAI extend into the tropical North Atlantic along a horseshoe pathway, with the largest signal remaining in the SPNA (Figure 1a). This is similar to the previously identified AMV SST pattern (e.g., Drews & Greatbatch, 2017; Frankignoul et al., 2017; Ruiz-Barradas et al., 2013) and different from the tripolar SST pattern induced by the North Atlantic Oscillation at interannual timescales (Delworth et al., 2017; Deser et al., 2010; Kushnir, 1994; Marshall et al., 2001; Visbeck et al., 2003). The observed SSS anomalies associated with MAI have an opposite sign over a latitudinal band in the tropical North Atlantic to that in the SPNA (Figure 1b), due to the northward shift of the Atlantic Intertropical Convergence Zone (ITCZ) and enhanced Sahel rainfall associated with a positive AMV phase and vice versa (Friedman et al., 2017). The observed UOHC pattern associated with the MAI (Figure 1c) is similar to the extratropical AMOC fingerprint pattern (Figure S1), that is, a dipole structure with opposite signs in the SPNA and the Gulf Stream region (Joyce & Zhang, 2010; Yan et al., 2017, 2018; Zhang, 2008, 2017; Zhang & Zhang, 2015), suggesting that the observed MAI is linked to AMOC variability. The observed MAI (Figure 1e) does not exhibit much high frequency variability and is very similar to its low-pass filtered component. It significantly correlates ($p < 0.05$) with multiple observed AMV-related SPNA indices (Figures 2a–2d) and the observed basin-wide SST-based AMV index (Figure 2e), all being linearly detrended. This is consistent with the previously identified high coherence among observed SPNA SST, SSS, UOHC, and UOSC associated with AMV at multidecadal timescales (Zhang, 2017). The above results confirm the capability of MEOF to extract AMV in observations.

In contrast, the spatial patterns (Figures 1f–1i) associated with the CMIP5 externally forced MAI (Figure 1j) obtained with linear detrending are very different from those observed (Figures 1a–1d), although the simulated MAI itself exhibits almost in-phase multidecadal variations compared to the observed MAI (Figures 1e and 1j). During the positive MAI phase, there is externally forced freshening in the SPNA (Figures 1g and 1i), opposite to that observed (Figures 1b and 1d); and the observed warming in the SPNA (Figure 1a) is missing in the externally forced SST pattern (Figure 1f), although there is a broad warming in lower latitudes outside the SPNA. In the Gulf Stream region, the simulated UOHC pattern during the positive MAI phase (Figure 1h) exhibits a warming signal that is opposite to that observed (Figure 1c).

The CMIP5 externally forced SPNA SST and UOHC indices (Figures 2f and 2h) show variations at much shorter timescales with much smaller amplitudes than those observed (Figures 2a and 2c). The CMIP5 externally forced SPNA SSS and UOSC indices (Figures 2g and 2i) are opposite to those observed (Figures 2b and 2d). The above externally forced AMV-related indices (Figures 2f–2i) do not have significant positive correlations with the externally forced MAI (Figure 1j) and with the linearly detrended basin-wide SST-based AMV index (Figure 2j), inconsistent with the previously identified high coherences among observed AMV-related SPNA temperature and salinity anomalies at multidecadal timescales (Zhang, 2017). The CMIP5 externally forced linearly detrended basin-wide SST-based AMV index (Figure 2j) seems consistent with that observed (Figure 2e) and with the externally forced MAI (Figure 1j), and represents the simulated wide-spread SST signal at low latitudes outside the SPNA (Figure 1f). However, we will show in the next section that this is an artifact of linear detrending and essentially reflects the component of the simulated global mean-correlated externally forced signal that deviates from a linear trend; it does not reflect a local process that is unique to the Atlantic.

## 4. Importance of Removing the Signal Associated With Global Mean SST for Analyzing AMV

When the signals regressed on global mean SST are removed, the observed MAI (Figure 3e), associated patterns (Figures 3a–3d), AMV-related indices (Figures 2k–2n), and basin-wide SST-based AMV index (Figure 2o) of the residual fields are all very similar to those obtained with linear detrending (Figures 1a–1e and 2a–2e). Again, the observed MAI (Figure 3e) significantly correlates ($p < 0.05$) with the observed

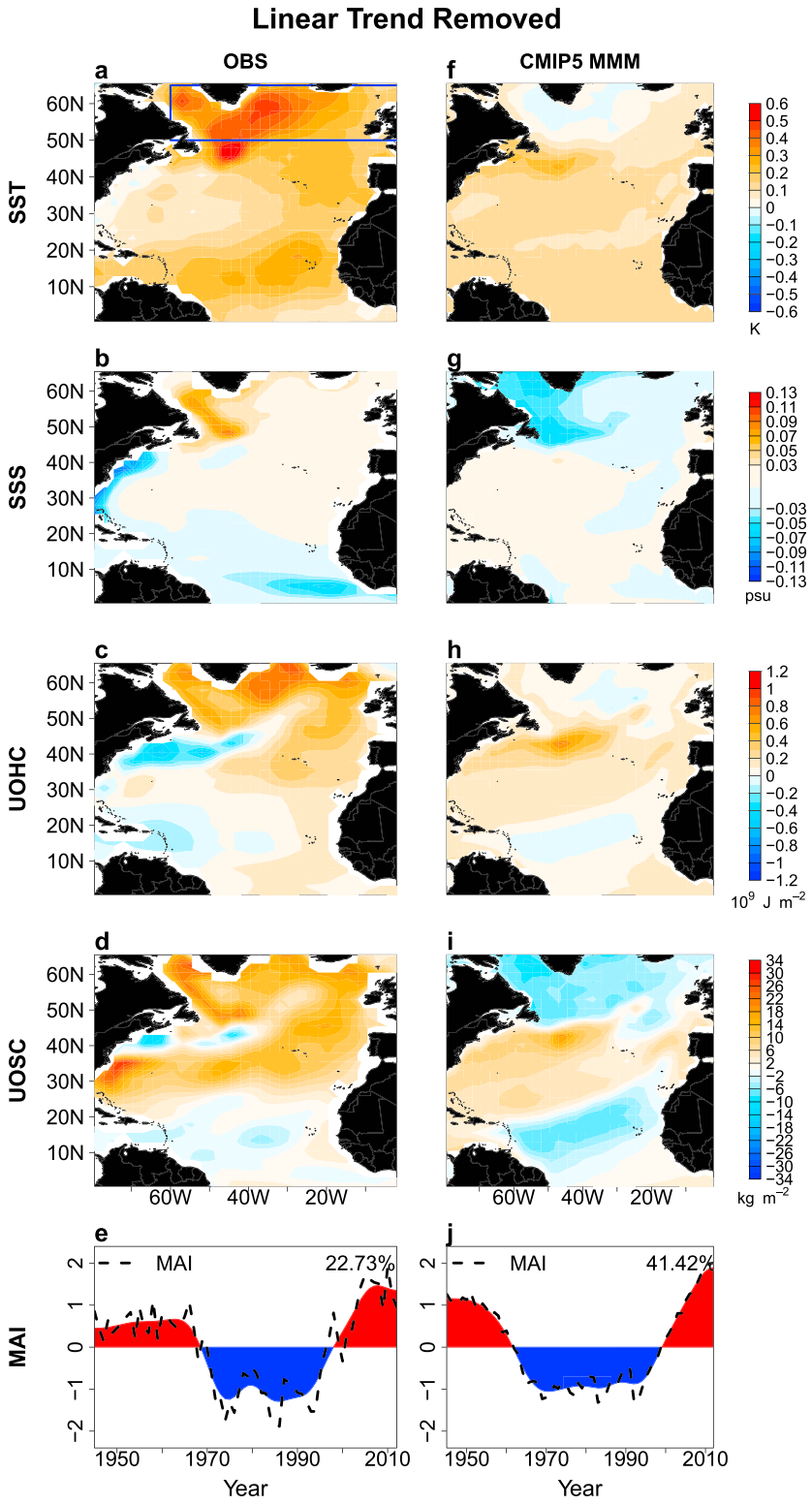


**Figure 1.** MAI and associated spatial patterns, with linear detrending. (a–d) Observed MAI patterns for (a) SST, (b) SSS, (c) UOHC, and (d) UOSC. (e) Observed MAI (dashed) and 10-year low-pass filtered component (red-blue shading). (f–j) same as (a–e) except for CMIP5 MMM. MAI explained variance is included in (e) and (j). Blue box in (a) marks the subpolar North Atlantic. SST = sea surface temperature; SSS = sea surface salinity; UOHC = upper ocean heat content; UOSC = upper ocean salt content; MAI = multivariate Atlantic Multidecadal Variability index; CMIP5 = Coupled Model Intercomparison Project Phase 5; MMM = multimodel mean.

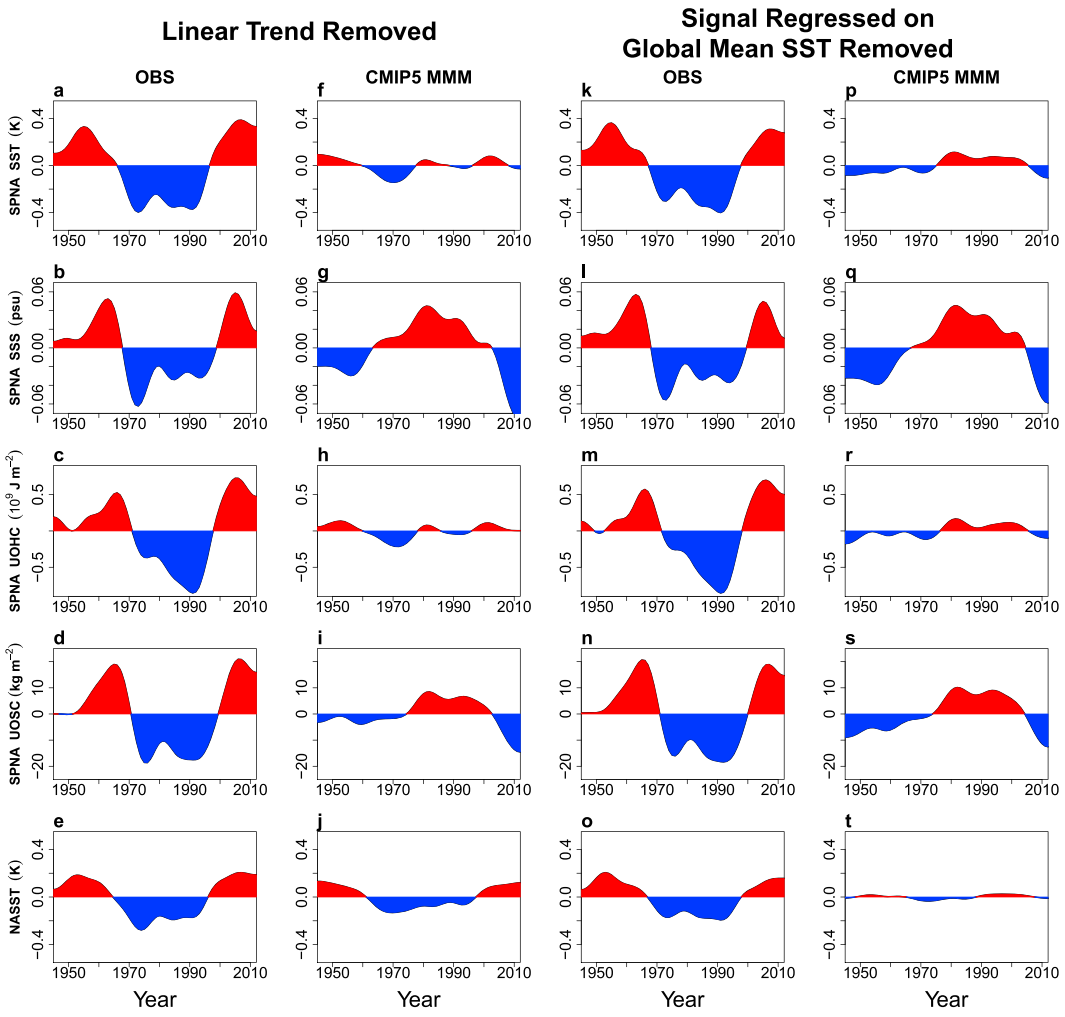


**Figure 2.** Low-pass filtered indices. (a–j) (left two columns) Linear detrending. (k–t) (right two columns) Signal regressed on global mean SST is removed. (a–e) and (k–o) (first and third columns) observations. (f–j) and (p–t) (second and fourth columns) CMIP5 MMM. Indices averaged over SPNA are shown in the first four rows: (a, f, k, and p) SST, (b, g, i, and q) SSS, (c, h, m, and r) UOHC, (d, i, n, and s) UOSC. SST index averaged over the North Atlantic (NASST) are shown in the last row (e, j, o, and t). SPNA = subpolar North Atlantic; SST = sea surface temperature; SSS = sea surface salinity; UOHC = upper ocean heat content; UOSC = upper ocean salt content; CMIP5 = Coupled Model Intercomparison Project Phase 5; MMM = multimodel mean.

AMV-related indices (Figures 2k–2n) and the observed basin-wide SST-based AMV index (Figure 2o). This insensitivity to detrending methods occurs because the observed global mean SST anomaly does not differ substantially from a linear trend and exhibits less multidecadal variability (Figure S2f) than the observed North Atlantic signal (Figures S2a–S2e). Hence, removing the signal regressed on global mean SST clearly illustrates that the observed AMV is indeed due to a local process that is unique to the Atlantic.

In contrast to observations, when the signal regressed on global mean SST is removed from the CMIP5 simulations, the residual spatial temperature patterns (Figures 3f and 3h) associated with the CMIP5 externally forced MAI (Figure 3j) are very different from those obtained with linear detrending (Figures 1f and 1h). During the positive MAI phase, the cooling in the SPNA becomes more pronounced and the broad warming in lower latitudes outside the SPNA is mostly missing in the associated externally forced SST and UOHC patterns (Figures 3f and 3h), compared with their linearly detrended counterparts (Figures 1f and 1h). Hence, the basin-wide temperature signal obtained with linear detrending (Figures 1f and 1h) mostly reflects the externally forced global mean-correlated signal that deviates from the linear trend, rather than being due to a local process that is unique to the Atlantic. The externally forced SSS and UOSC patterns are less

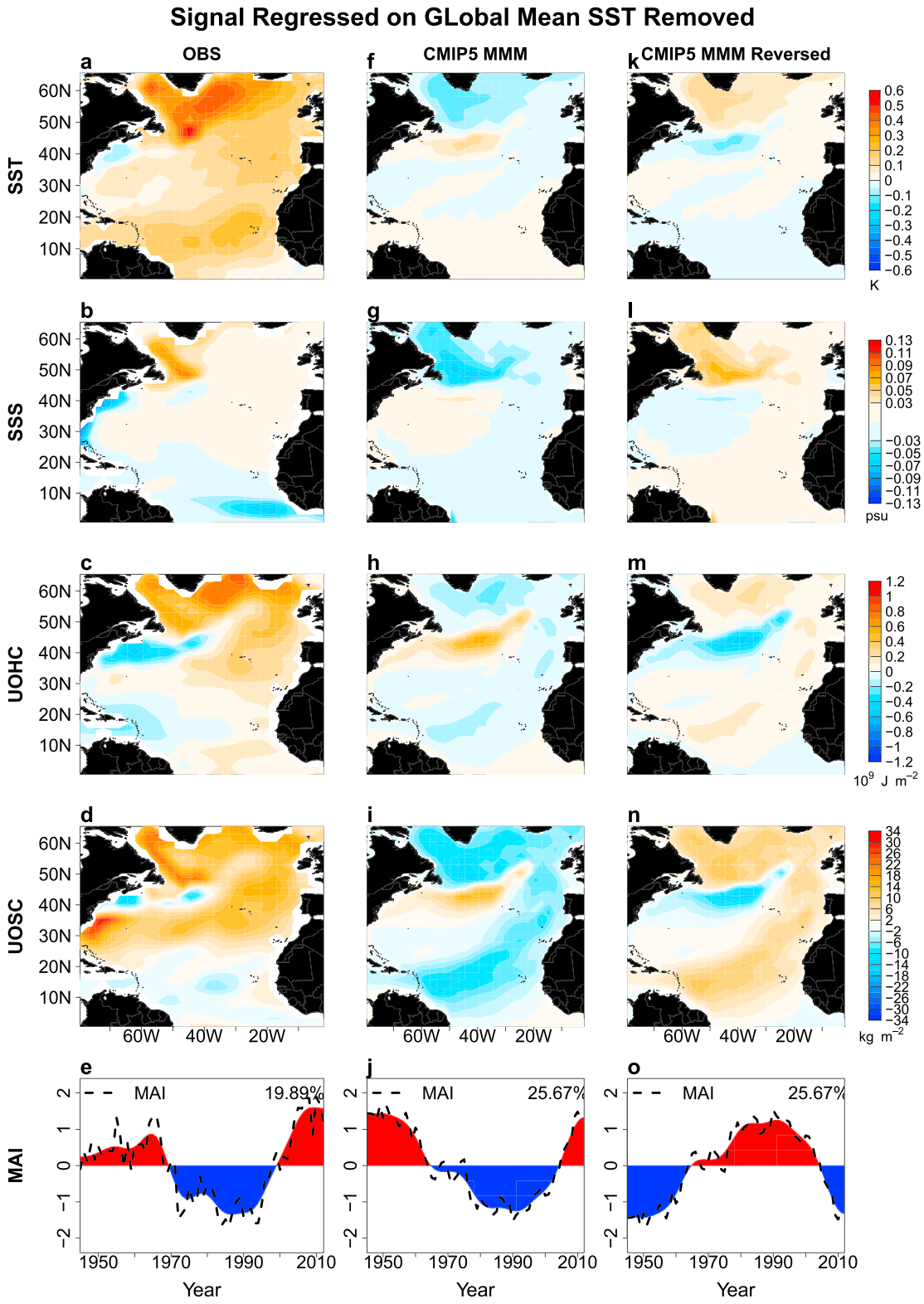


**Figure 3.** MAI and associated spatial patterns, with the signal regressed on global mean SST removed. (a–d) Observed MAI patterns for (a) SST, (b) SSS, (c) UOHC, and (d) UOSC. (e) Observed MAI (dashed) and 10-year low-pass filtered component (red-blue shading). (f–j) same as (a–e) except for CMIP5 MMM. (k–o) same as (f–j) except that signs are flipped. MAI explained variance is included in (e, j, and o). SST = sea surface temperature; SSS = sea surface salinity; UOHC = upper ocean heat content; UOSC = upper ocean salt content; MAI = multivariate Atlantic Multidecadal Variability index; CMIP5 = Coupled Model Intercomparison Project Phase 5; MMM = multimodel mean.

sensitive to detrending methods, and those obtained with nonlinear detrending exhibit a similar freshening in the SPNA during positive MAI phases (Figures 3g and 3i) compared to their linearly detrended counterparts (Figures 1g and 1i), which remains opposite to observations (Figures 3b and 3d). When the signal regressed on global mean SST is removed, each residual spatial pattern (Figures 3f–3i) associated with the CMIP5 externally forced MAI (Figure 3j) exhibits a negative spatial correlation with that observed (Figures 3a–3d) over the entire North Atlantic. We reversed the sign of the MAI (Figure 3o) and associated spatial patterns (Figures 3k–3n), so that the spatial patterns associated with the reversed MAI all have positive spatial correlations with those observed (Figures 3a–3d) over the entire North Atlantic, and the reversed MAI (Figure 3o) can better represent the phase of this simulated AMV and reveal its disagreement with that observed (Figure 3e).

Similarly, when the signal regressed on global mean SST is removed, the residual CMIP5 externally forced SPNA SST and UOHC indices (Figures 2p and 2r) are now quite different from those obtained with linear detrending (Figures 2f and 2h) and exhibit antiphase multidecadal variations with their observed counterparts (Figures 2k and 2m). The residual CMIP5 externally forced SPNA SSS and UOSC indices (Figures 2q and 2s) remain similar to those obtained with linear detrending (Figures 2g and 2i) and opposite to those observed (Figures 2i and 2n). The above externally forced AMV-related indices (Figures 2p–2s) have significant ($p < 0.05$) positive correlations with each other and with the reversed externally forced MAI (Figure 3o), revealing a coherent externally forced multidecadal variability especially in the SPNA, but is opposite to observations. These results consistently suggest that the observed AMV is not dominated by external forcing. The residual CMIP5 externally forced basin-wide SST-based AMV index (Figure 2t), after removal of the signal regressed on global mean SST, also becomes quite different from that obtained with linear detrending (Figure 2j) and from that observed (Figure 2o), with a dramatically reduced and negligible amplitude. It is not significantly correlated with other externally forced AMV-related indices (Figures 2p–2s) and the reversed MAI (Figure 3o), that is, it is not a meaningful index for the coherent externally forced AMV. Hence, the CMIP5 externally forced linearly detrended basin-wide SST-based AMV index (Figure 2j) essentially reflects the global mean-correlated signal that deviates from a linear trend and is not unique to the Atlantic. This is confirmed by the high similarity between the CMIP5 externally forced low-pass filtered North Atlantic mean SST and global mean SST anomalies without any detrending (Figures S2k and S2l), whereas their observed counterparts are quite different from each other (Figures S2e and S2f).

## 5. Relationship Between AMV and AMOC Fingerprint

For both detrending methods, the observed AMOC fingerprint exhibits a similar dipole pattern with opposite signs in the SPNA and the Gulf Stream region (Figures 4a and 4e) and similar multidecadal variations (Figures 4b and 4f), as found in previous studies (Joyce & Zhang, 2010; Yan et al., 2017, 2018; Zhang, 2008, 2017; Zhang & Zhang, 2015). The low-pass filtered observed AMOC fingerprint (Figures 4b and 4f) has significant ($p < 0.05$) positive correlations with various observed AMV-related indices (Figures 2a–2e and 2k–2o) and the observed MAI (Figures 1e and 3e), for both detrending methods. This is also consistent with previous studies (Yan et al., 2018; Zhang, 2017) and supports the interpretation that the observed AMV is closely linked to the AMOC variability.

For the CMIP5 externally forced response, the AMOC fingerprint is significantly ($p < 0.05$) correlated with the detrended AMOC index at low frequency, with positive anomalies from 1970s to 1990s and negative anomalies before and afterward for both detrending methods (Figures 4d and 4h). This detrended forced multidecadal AMOC variability is similar to that reported in previous studies (Cheng et al., 2013; Kim, Yeager, Chang, et al., 2018; Menary et al., 2013; Tandon & Kushner, 2015), but is almost antiphase with that indicated by the observed AMOC fingerprint (Figures 4b and 4f). With linear detrending, the forced AMOC fingerprint pattern is centered around the Gulf Stream region (Figure 4c). When the signal regressed on global mean SST is removed, the forced AMOC fingerprint pattern (Figure 4g) is improved and becomes more similar to that observed (with a positive spatial correlation), but the subpolar signal remains weak (likely related to different locations of the subpolar signal in different models). The detrended forced multidecadal AMOC variability also has a small amplitude (Figure 4h) compared to that of the internal multidecadal AMOC variability in some CMIP5 control simulations and the observational-based estimate (Yan et al.,

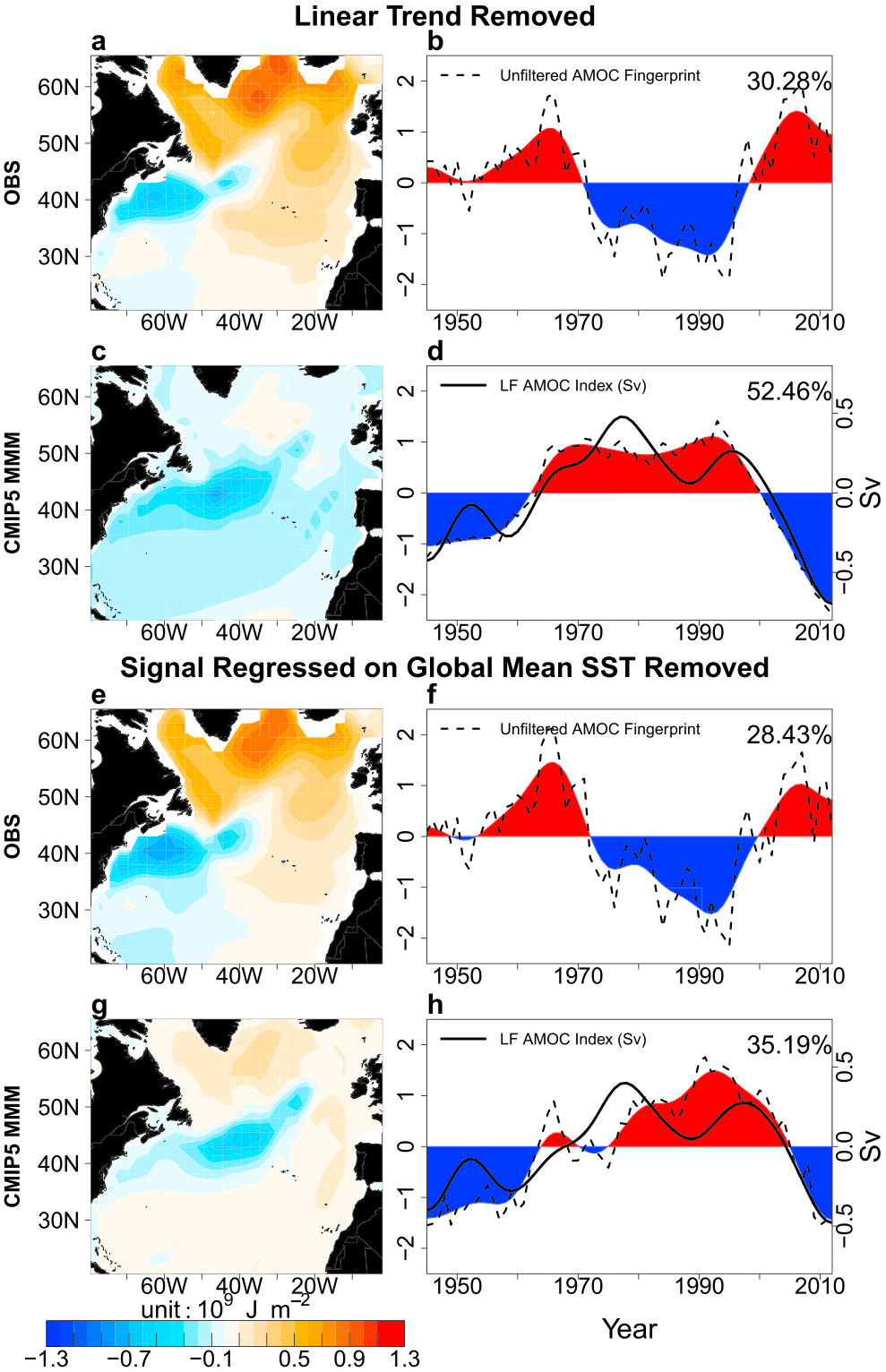


**Figure 4.** AMOC fingerprints (i.e., leading mode of upper ocean heat content in the extratropical North Atlantic). (a–d) (upper two rows) Linear detrending. (e–h) (lower two rows) Signal regressed on global mean SST is removed. (first and third rows) Observed AMOC fingerprint pattern (a and e) and corresponding time series (normalized leading principal component PC1, dashed) and 10-year low-pass filtered component (red-blue shading) (b and f). Second and fourth rows (c, d, g, and h): same as (a), (b), (e), and (f), except for CMIP5 MMM. Explained variance by the leading mode is included in (b), (d), (f), and (h). Also included in (d) and (h) is 10-year low-pass filtered CMIP5 MMM AMOC index at 26°N (black, Sv, right axis). CMIP5 = Coupled Model Intercomparison Project Phase 5; MMM = multimodel mean; AMOC = Atlantic Meridional Overturning Circulation; SST = sea surface temperature.

2018), and this may also contribute to the weak dipole signal in the forced AMOC fingerprint pattern (Figure 4g).

With linear detrending, the CMIP5 forced low-pass filtered AMOC index (Figure 4d) has significant ($p < 0.05$) positive correlations with the forced AMV-related subpolar SSS/UOSC indices (Figures 2g or 2i), but not with the forced subpolar SST/UOHC indices (Figures 2f or 2h) and is anticorrelated with the forced MAI (Figure 1j) and the basin-wide SST-based AMV index (Figure 2j). When the signal regressed on global mean SST is removed, the residual forced low-pass filtered AMOC index (or AMOC fingerprint; Figure 4h) has significant ($p < 0.05$) positive correlations with the residual forced AMV-related SPNA indices (Figures 2p–2s) and the reversed MAI (Figure 3o), and no relationship with the residual forced basin-wide SST-based AMV index which is negligible (Figure 2t). This is consistent with the positive correlations between AMOC and AMV-related SPNA temperature and salinity anomalies found in many CMIP5 control simulations (e.g., Yan et al., 2018). Both the residual CMIP5 externally forced AMOC fingerprint (Figure 4h) and AMV signal (Figures 2p–2s and 3o) are almost in antiphase with their observed counterparts (Figures 4f, 2k–2n, and 3e).

## 6. Conclusion and Discussion

The MAI and associated spatial patterns provide a multivariate measure of AMV. The MEOF approach has the advantage of extracting AMV without low-pass time filtering. The method is not limited to the four variables used in this study and can in future studies include other variables that have high coherences with AMV only at low frequency. Coherent multidecadal variability that is unique to the Atlantic is found in the observed MAI, various AMV-related indices, and the AMOC fingerprint. In CMIP5 simulations, when the signal associated with global mean SST is removed, coherent residual externally forced multidecadal variability is identified in the reversed MAI, AMV-related SPNA indices, AMOC fingerprint, and AMOC index. However, these signals disagree strongly with observations, suggesting that the observed multidecadal AMOC variability inferred from its fingerprint and the associated observed AMV are not dominated by external forcing. This contrasts with the conclusions of some previous studies based on linear detrending (e.g., Bellomo et al., 2018; Bellucci et al., 2017; Booth et al., 2012; Murphy et al., 2017).

Our results demonstrate that the resemblance between linearly detrended observed and CMIP5 forced basin-wide SST-based AMV indices is an artifact of the linear detrending method. The anticorrelation between the linearly detrended CMIP5 forced basin-wide SST-based AMV index and multidecadal AMOC variations, as found in previous studies (Cheng et al., 2013; Tandon & Kushner, 2015), is also an artifact of linear detrending and does not depict a relationship between AMOC and the local variability that is unique to the Atlantic. It essentially reflects the relationship between a linearly detrended forced global mean-correlated signal and multidecadal AMOC variability. That is, a forced global warming (cooling) is associated with an AMOC weakening (strengthening) as often found in climate models (e.g., Delworth & Dixon, 2006; Gregory et al., 2005; Manabe et al., 1991; Meehl et al., 2007). With the global mean-correlated signal removed, the residual CMIP5 forced basin-wide SST-based AMV index also disagrees strongly with the observed residual, with the latter retaining a strong AMV signal. While the MEOF approach can extract a residual CMIP5 forced AMV signal that is unique to the Atlantic and in phase with the forced AMOC variability, this signal is very different from observations. In summary, our findings suggest that the observed AMV is not dominated by external forcing.

**Acknowledgments**
Yan is funded by Princeton University's Cooperative Institute for Modeling the Earth System. We acknowledge the World Climate Research Programme's Working Group on Coupled Modeling, which is responsible for CMIP, and we thank the climate modeling groups for producing and making available their model output. For CMIP, the U.S. Department of Energy's Program for Climate Model Diagnosis and Intercomparison provides coordinated support and led development of a software infrastructure in partnership with the Global Organization for Earth System Science Portals. We thank Liwei Jia and Xiaosong Yang for their comments on the manuscript. The findings are those of the authors and do not necessarily reflect the views of NOAA, U.S. Government, or other funding institutions. The Ishii data used in this study can be downloaded online (from https://rda.ucar.edu/datasets/ds285.3/), the HadISST1.1 data set used in this study can be downloaded online (from https://www.metoffice.gov.uk/hadobs/hadisst/), and the CMIP3/CMIP5 model output used in this study can be downloaded online (from https://esgf-node.llnl.gov/projects/esgf-llnl/).

## References

Ba, J., Keenlyside, N. S., Latif, M., Park, W., Ding, H., Lohmann, K., et al. (2014). A multi-model comparison of Atlantic multidecadal variability. *Climate Dynamics*, *43*(9-10), 2333–2348. https://doi.org/10.1007/s00382-014-2056-1

Ba, J., Keenlyside, N. S., Park, W., Latif, M., Hawkins, E., & Ding, H. (2013). A mechanism for Atlantic multidecadal variability in the Kiel Climate Model. *Climate Dynamics*, *41*(7-8), 2133–2144. https://doi.org/10.1007/s00382-012-1633-4

Bellomo, K., Murphy, L. N., Cane, M. A., Clement, A. C., & Polvani, L. M. (2018). Historical forcings as main drivers of the Atlantic multidecadal variability in the CESM large ensemble. *Climate Dynamics*, *50*(9-10), 3687–3698. https://doi.org/10.1007/s00382-017-3834-3

Bellucci, A., Mariotti, A., & Gualdi, S. (2017). The role of forcings in the twentieth-century North Atlantic multidecadal variability: The 1940–75 North Atlantic cooling case study. *Journal of Climate*, *30*(18), 7317–7337. https://doi.org/10.1175/JCLI-D-16-0301.1

Booth, B. B., Dunstone, N. J., Halloran, P. R., Andrews, T., & Bellouin, N. (2012). Aerosols implicated as a prime driver of twentieth-century North Atlantic climate variability. *Nature*, *484*(7393), 228–232. https://doi.org/10.1038/nature10946

Chen, X., & Tung, K. K. (2014). Varying planetary heat sink led to global-warming slowdown and acceleration. *Science*, *345*(6199), 897–903. https://doi.org/10.1126/science.1254937

Chen, X., & Tung, K. K. (2018). Global surface warming enhanced by weak Atlantic overturning circulation. *Nature*, *559*(7714), 387–391. https://doi.org/10.1038/s41586-018-0320-y

Cheng, W., Chiang, J. C. H., & Zhang, D. (2013). Atlantic meridional overturning circulation (AMOC) in CMIP5 models: RCP and historical simulations. *Journal of Climate*, *26*(18), 7187–7197. https://doi.org/10.1175/JCLI-D-12-00496.1

Delworth, T. L., & Dixon, K. W. (2006). Have anthropogenic aerosols delayed a greenhouse gas-induced weakening of the North Atlantic thermohaline circulation? *Geophysical Research Letters*, *33*, L02606. https://doi.org/10.1029/2005GL024980

Delworth, T. L., & Mann, M. E. (2000). Observed and simulated multidecadal variability in the Northern Hemisphere. *Climate Dynamics*, *16*(9), 661–676. https://doi.org/10.1007/s003820000075

Delworth, T. L., Zeng, F., Zhang, L., Zhang, R., Vecchi, G. A., & Yang, X. (2017). The central role of ocean dynamics in connecting the North Atlantic Oscillation to the extratropical component of the Atlantic Multidecadal Oscillation. *Journal of Climate*, *30*(10), 3789–3805. https://doi.org/10.1175/JCLI-D-16-0358.1

Deser, C., Alexander, M. A., Xie, S. P., & Phillips, A. S. (2010). Sea surface temperature variability: Patterns and mechanisms. *Annual Review of Marine Science*, *2*(1), 115–143. https://doi.org/10.1146/annurev-marine-120408-151453

Drews, A., & Greatbatch, R. J. (2016). Atlantic multidecadal variability in a model with an improved North Atlantic current. *Geophysical Research Letters*, *43*, 8199–8206. https://doi.org/10.1002/2016GL069815

Drews, A., & Greatbatch, R. J. (2017). Evolution of the Atlantic multidecadal variability in a model with an improved North Atlantic current. *Journal of Climate*, *30*(14), 5491–5512. https://doi.org/10.1175/JCLI-D-16-0790.1

Ebisuzaki, W. (1997). A method to estimate the statistical significance of a correlation when the data are serially correlated. *Journal of Climate*, *10*(9), 2147–2153. https://doi.org/10.1175/1520-0442(1997)010<2147:AMTETS>2.0.CO;2

Enfield, D. B., Mestas-Nuñez, A. M., & Trimble, P. J. (2001). The Atlantic multidecadal oscillation and its relation to rainfall and river flows in the continental US. *Geophysical Research Letters*, *28*(10), 2077–2080. https://doi.org/10.1029/2000GL012745

Frajka-Williams, E., Beaulieu, C., & Duchez, A. (2017). Emerging negative Atlantic Multidecadal Oscillation index in spite of warm subtropics. *Scientific Reports*, *7*(1), 11224. https://doi.org/10.1038/s41598-017-11046-x

Frankcombe, L. M., England, M. H., Mann, M. E., & Steinman, B. A. (2015). Separating internal variability from the externally forced climate response. *Journal of Climate*, *28*(20), 8184–8202. https://doi.org/10.1175/JCLI-D-15-0069.1

Frankignoul, C., Gastineau, G., & Kwon, Y. O. (2017). Estimation of the SST response to anthropogenic and external forcing and its impact on the Atlantic Multidecadal Oscillation and the Pacific Decadal Oscillation. *Journal of Climate*, *30*(24), 9871–9895. https://doi.org/10.1175/JCLI-D-17-0009.1

Friedman, A. R., Reverdin, G., Khodri, M., & Gastineau, G. (2017). A new record of Atlantic sea surface salinity from 1896 to 2013 reveals the signatures of climate variability and long-term trends. *Geophysical Research Letters*, *44*, 1866–1876. https://doi.org/10.1002/2017GL072582

Fukumori, I., & Wunsch, C. (1991). Efficient representation of the North Atlantic hydrographic and chemical distributions. *Progress in Oceanography*, *27*(1-2), 111–195. https://doi.org/10.1016/0079-6611(91)90015-E

Gregory, J. M., Dixon, K. W., Stouffer, R. J., Weaver, A. J., Driesschaert, E., Eby, M., et al. (2005). A model intercomparison of changes in the Atlantic thermohaline circulation in response to increasing atmospheric $CO_2$ concentration. *Geophysical Research Letters*, *32*, L12703. https://doi.org/10.1029/2005GL023209

Ishii, M., Kimoto, M., Sakamoto, K., & Iwasaki, S. I. (2006). Steric sea level changes estimated from historical ocean subsurface temperature and salinity analyses. *Journal of Oceanography*, *62*(2), 155–170. https://doi.org/10.1007/s10872-006-0041-y

Joyce, T. M., & Zhang, R. (2010). On the path of the Gulf Stream and the Atlantic meridional overturning circulation. *Journal of Climate*, *23*(11), 3146–3154. https://doi.org/10.1175/2010JCLI3310.1

Kajtar, J. B., Collins, M., Frankcombe, L. M., England, M. H., Osborn, T. J., & Juniper, M. (2019). Global mean surface temperature response to large-scale patterns of variability in observations and CMIP5. *Geophysical Research Letters*, *46*, 2232–2241. https://doi.org/10.1029/2018GL081462

Kavvada, A., Ruiz-Barradas, A., & Nigam, S. (2013). AMO's structure and climate footprint in observations and IPCC AR5 climate simulations. *Climate Dynamics*, *41*(5-6), 1345–1364. https://doi.org/10.1007/s00382-013-1712-1

Kim, W. M., Yeager, S., Chang, P., & Danabasoglu, G. (2018). Low-frequency North Atlantic climate variability in the Community Earth System Model large ensemble. *Journal of Climate*, *31*(2), 787–813. https://doi.org/10.1175/JCLI-D-17-0193.1

Kim, W. M., Yeager, S. G., & Danabasoglu, G. (2018). Key role of internal ocean dynamics in Atlantic multidecadal variability during the last half century. *Geophysical Research Letters*, *45*, 13,449–13,457. https://doi.org/10.1029/2018GL080474

Knight, J. R., Allan, R. J., Folland, C. K., Vellinga, M., & Mann, M. E. (2005). A signature of persistent natural thermohaline circulation cycles in observed climate. *Journal of Geophysical Research*, *32*, L20708. https://doi.org/10.1029/2005GL024233

Kushnir, Y. (1994). Interdecadal variations in North Atlantic sea surface temperature and associated atmospheric conditions. *Journal of Climate*, *7*(1), 141–157. https://doi.org/10.1175/1520-0442(1994)007<0141:IVINAS>2.0.CO;2

Kutzbach, J. E. (1967). Empirical eigenvectors of sea-level pressure, surface temperature and precipitation complexes over North America. *Journal of Applied Meteorology*, *6*(5), 791–802. https://doi.org/10.1175/1520-0450(1967)006<0791:EEOSLP>2.0.CO;2

Latif, M., Böning, C., Willebrand, J., Biastoch, A., Dengg, J., Keenlyside, N., et al. (2006). Is the thermohaline circulation changing? *Journal of Climate*, *19*(18), 4631–4637. https://doi.org/10.1175/JCLI3876.1

Manabe, S., Stouffer, R. J., Spelman, M. J., & Bryan, K. (1991). Transient responses of a coupled ocean-atmosphere model to gradual changes of atmospheric $CO_2$. Part 1. Annual mean response. *Journal of Climate*, *4*(8), 785–818. https://doi.org/10.1175/1520-0442(1991)004<0785:TROACO>2.0.CO;2

Marshall, J., Kushnir, Y., Battisti, D., Chang, P., Czaja, A., Dickson, R., et al. (2001). North Atlantic climate variability: Phenomena, impacts and mechanisms. *International Journal of Climatology*, *21*(15), 1863–1898. https://doi.org/10.1002/joc.693

McCarthy, G. D., Haigh, I. D., Hirschi, J. J. M., Grist, J. P., & Smeed, D. A. (2015). Ocean impact on decadal Atlantic climate variability revealed by sea-level observations. *Nature*, *521*(7553), 508–510. https://doi.org/10.1038/nature14491

Meehl, G. A., Stocker, T. F., Collins, W. D., Friedlingstein, P., Gaye, A. T., Gregory, J. M., et al. (2007). Global climate projections. In S. Solomon, D. Qin, M. Manning, Z. Chen, M. Marquis, K. B. Averyt, M. Tignor, & H. L. Miller (Eds.), *Climate change 2007: The physical science basis. Contribution of Working Group I to the Fourth Assessment Report of the Intergovernmental Panel on Climate Change* (pp. 747–845). Cambridge, UK: Cambridge University Press.

Menary, M. B., Roberts, C. D., Palmer, M. D., Halloran, P. R., Jackson, L., Wood, R. A., et al. (2013). Mechanisms of aerosol-forced AMOC variability in a state of the art climate model. *Journal of Geophysical Research: Oceans*, *118*, 2087–2096. https://doi.org/10.1002/jgrc.20178

Murphy, L. N., Bellomo, K., Cane, M., & Clement, A. (2017). The role of historical forcings in simulating the observed Atlantic multidecadal oscillation. *Geophysical Research Letters*, *44*, 2472–2480. https://doi.org/10.1002/2016GL071337

Park, T., Park, W., & Latif, M. (2016). Correcting North Atlantic sea surface salinity biases in the Kiel climate model: Influences on ocean circulation and Atlantic multidecadal variability. *Climate Dynamics*, *47*(7-8), 2543–2560. https://doi.org/10.1007/s00382-016-2982-1

Rayner, N. A., Parker, D. E., Horton, E. B., Folland, C. K., Alexander, L. V., Rowell, D. P., et al. (2003). Global analyses of sea surface temperature, sea ice, and night marine air temperature since the late nineteenth century. *Journal of Geophysical Research*, *108*(D14), 4407. https://doi.org/10.1029/2002JD002670

Robson, J., Ortega, P., & Sutton, R. (2016). A reversal of climatic trends in the North Atlantic since 2005. *Nature Geoscience*, *9*(7), 513–517. https://doi.org/10.1038/ngeo2727

Robson, J., Sutton, R., Lohmann, K., Smith, D., & Palmer, M. (2012). Causes of the rapid warming of the North Atlantic Ocean in the mid-1990s. *Journal of Climate*, *25*(12), 4116–4134. https://doi.org/10.1175/JCLI-D-11-00443.1

Ruiz-Barradas, A., Nigam, S., & Kavvada, A. (2013). The Atlantic Multidecadal Oscillation in twentieth century climate simulations: Uneven progress from CMIP3 to CMIP5. *Climate Dynamics*, *41*(11-12), 3301–3315. https://doi.org/10.1007/s00382-013-1810-0

Smeed, D. A., Josey, S. A., Beaulieu, C., Johns, W. E., Moat, B. I., Frajka-Williams, E., et al. (2018). The North Atlantic Ocean is in a state of reduced overturning. *Geophysical Research Letters*, *45*, 1527–1533. https://doi.org/10.1002/2017GL076350

Smeed, D. A., McCarthy, G. D., Cunningham, S. A., Frajka-Williams, E., Rayner, D., Johns, W. E., et al. (2014). Observed decline of the Atlantic Meridional Overturning Circulation 2004–2012. *Ocean Science*, *10*(1), 29–38. https://doi.org/10.5194/os-10-29-2014

Sparnocchia, S., Pinardi, N., & Demirov, E. (2003). Multivariate empirical orthogonal function analysis of the upper thermocline structure of the Mediterranean Sea from observations and model simulations. *Annales Geophysicae*, *21*(1), 167–187. https://doi.org/10.5194/angeo-21-167-2003

Sutton, R. T., McCarthy, G. D., Robson, J., Sinha, B., Archibald, A. T., & Gray, L. J. (2018). Atlantic multidecadal variability and the UK ACSIS program. *Bulletin of the American Meteorological Society*, *99*(2), 415–425. https://doi.org/10.1175/BAMS-D-16-0266.1

Tandon, N. F., & Kushner, P. J. (2015). Does external forcing interfere with the AMOC's influence on North Atlantic sea surface temperature? *Journal of Climate*, *28*(16), 6309–6323. https://doi.org/10.1175/JCLI-D-14-00664.1

Trenberth, K. E., & Shea, D. J. (2006). Atlantic hurricanes and natural variability in 2005. *Geophysical Research Letters*, *33*, L12704. https://doi.org/10.1029/2006GL026894

Visbeck, M., Chassignet, E. P., Curry, R. G., Delworth, T. L., Dickson, R. R., & Krahmann, G. (2003). The ocean's response to North Atlantic oscillation variability. In *The North Atlantic oscillation: Climatic significance and environmental impact*, *Geophysical Monograph Series* (Vol. 134, pp. 113–145). Washington, DC: American Geophysical Union.

Wang, C., Dong, S., & Munoz, E. (2010). Seawater density variations in the North Atlantic and the Atlantic meridional overturning circulation. *Climate Dynamics*, *34*(7-8), 953–968. https://doi.org/10.1007/s00382-009-0560-5

Wolter, K., & Timlin, M. S. (1998). Measuring the strength of ENSO events—How does 1997/98 rank? *Weather*, *53*(9), 315–324. https://doi.org/10.1002/j.1477-8696.1998.tb06408.x

Wolter, K., & Timlin, M. S. (2011). El Niño/Southern Oscillation behaviour since 1871 as diagnosed in an extended multivariate ENSO index (MEI.ext). *International Journal of Climatology*, *31*(7), 1074–1087. https://doi.org/10.1002/joc.2336

Yan, X., Zhang, R., & Knutson, T. R. (2017). The role of Atlantic overturning circulation in the recent decline of Atlantic major hurricane frequency. *Nature Communications*, *8*(1), 1695. https://doi.org/10.1038/s41467-017-01377-8

Yan, X., Zhang, R., & Knutson, T. R. (2018). Underestimated AMOC variability and implications for AMV and predictability in CMIP models. *Geophysical Research Letters*, *45*, 4319–4328. https://doi.org/10.1029/2018GL077378

Yeager, S., & Danabasoglu, G. (2014). The origins of late-twentieth-century variations in the large-scale North Atlantic circulation. *Journal of Climate*, *27*(9), 3222–3247. https://doi.org/10.1175/JCLI-D-13-00125.1

Zhang, J., & Zhang, R. (2015). On the evolution of Atlantic meridional overturning circulation fingerprint and implications for decadal predictability in the North Atlantic. *Geophysical Research Letters*, *42*, 5419–5426. https://doi.org/10.1002/2015GL064596

Zhang, R. (2007). Anticorrelated multidecadal variations between surface and subsurface tropical North Atlantic. *Geophysical Research Letters*, *34*, L12713. https://doi.org/10.1029/2007GL030225

Zhang, R. (2008). Coherent surface-subsurface fingerprint of the Atlantic meridional overturning circulation. *Geophysical Research Letters*, *35*, L20705. https://doi.org/10.1029/2008GL035463

Zhang, R. (2017). On the persistence and coherence of subpolar sea surface temperature and salinity anomalies associated with the Atlantic multidecadal variability. *Geophysical Research Letters*, *44*, 7865–7875. https://doi.org/10.1002/2017GL074342

Zhang, R., Delworth, T. L., Sutton, R., Hodson, D. L. R., Dixon, K. W., Held, I. M., et al. (2013). Have aerosols caused the observed Atlantic multidecadal variability. *Journal of the Atmospheric Sciences*, *70*(4), 1135–1144. https://doi.org/10.1175/JAS-D-12-0331.1

Zhang, R., Sutton, R., Danabasoglu, G., Delworth, T. L., Kim, W. M., Robson, J., & Yeager, S. G. (2016). Comment on "The Atlantic Multidecadal Oscillation without a role for ocean circulation". *Science*, *352*(6293), 1527–1527. https://doi.org/10.1126/science.aaf1660